

A Bandpass Twin-T Active Filter Used in the Buchla 200 Electric Music Box Synthesizer

Aaron D. Lanterman

Abstract—This paper analyzes an unusual active bandpass filter employed in the Buchla Model 295 10 Channel Comb Filter, a synthesizer module developed as part of the Buchla 200 Electric Music Box by Donald Buchla. The filter consists of a peculiar rearrangement of elements in a classic Twin-T configuration; to our knowledge, it has not been previously addressed in the literature. As an example, we explore its specific application in the Model 295.

Index Terms—active filters, music synthesis

I. INTRODUCTION

The classic Twin-T circuit configuration is commonly used as a notch filter, in both passive and active implementations (see [1], [2] and pp. 288-290 of [3]). Figure 6.10 on p. 192 of [4], Figure 4(b) on p. 232 of [1], and Figure 1 on p. 46 of [5] employ a Twin-T network in the feedback loop of an inverting amplifier configuration to form a bandpass filter. Figure 1 shows a curious rearrangement of the Twin-T concept that acts as a bandpass filter in the Buchla Model 295 10 Channel Comb Filter,¹ one of the modules in the Buchla 200 Electric Music Box modular synthesizer system created by electronic music pioneer Donald Buchla [7] in the 1970s.

Figure 2 shows a passive variation, in which C_2 and R_2 are hooked to real ground instead of a virtual ground. If R_1 and C_3 are swapped, and C_1 and R_3 are swapped, it then resembles the traditional passive Twin-T notch filter; here it is drawn slightly differently than is typical to emphasize the resemblance to Figure 1. It can also be thought of as the traditional passive Twin-T notch filter with the ground and input connections swapped, as illustrated in Figure 1(a) of [1] (taking $V_1 = 0$ and V_2 as the input in that figure). A special case of this passive filter, with $2R_1 = R_2 = R_3$ and $C_1/2 = C_2 = C_3$, appears as Figure 8.34(a) on p. 467 of [8], with pin 3 of that figure acting as the input and pin 2 acting as the output, where it is named “Bandpass Twin-T.” Terry Watson stumbled across the same special case in his master’s thesis work when he accidentally swapped connections to a standard Twin-T network (Figure 16 on p. 35 of [9], with \bar{E}_2 of that figure acting as the input and \bar{E}_1 acting as the output). He suggests it “might be used as a lead-lag compensating network,” but does not explore it further.

To our knowledge, this paper is the first to analyze the inverting active bandpass topology of Figure 1; we have been unable to find any instances of it in the literature. A

School of Electrical Engineering, Georgia Institute of Technology, 777 Atlantic Drive, Atlanta, GA 30332 USA. E-mail: lanterma@ece.gatech.edu.

¹Buchla used the term “comb” somewhat loosely, as the bands are not equally spaced. They are instead organized along the lines of a “Bark” scale [6].

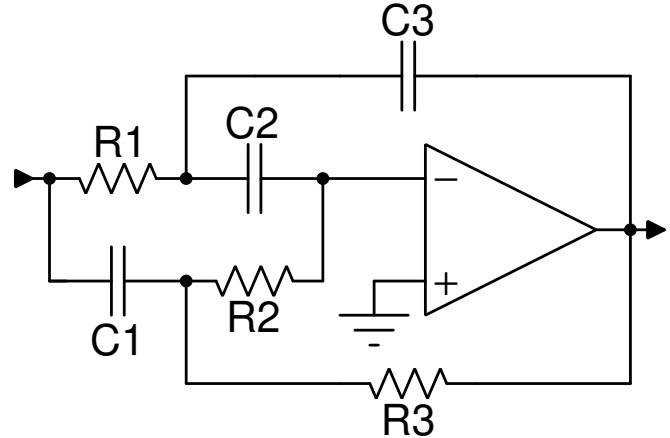


Fig. 1. Active bandpass filter used in the 200 Hz to 3.2 kHz filter blocks of Figure 3.

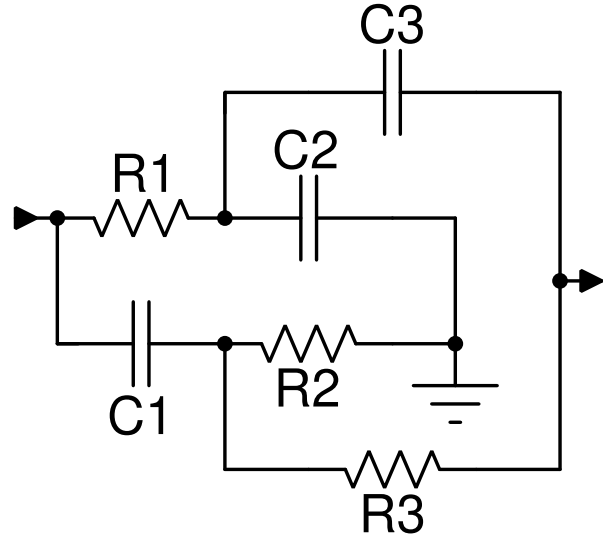


Fig. 2. Passive variant of the bandpass filter in Figure 2.

noninverting peaking filter may be derived by swapping the input and ground in Figure 1, but the gain of that noninverting filter cannot drop below unity [10], and hence it is not a strict bandpass filter.

MATLAB/Octave code to generate the plots in this paper may be found at <https://github.com/lantertronics/buchla-plots> under the name `b295_plots.m`.

TABLE I
BUCHLA MODEL 295 FILTERBANK PART VALUES

Band	$C_1 = C_3$	C_2	R_2	R'_2
200 Hz	47 nF	10 nF	68–168 k Ω	89.8 k Ω
350 Hz	22 nF	4.7 nF	91–191 k Ω	133 k Ω
500 Hz	22 nF	2.2 nF	91–191 k Ω	140 k Ω
700 Hz	10 nF	1.5 nF	150–250 k Ω	230 k Ω
1000 Hz	10 nF	910 pF	150–250 k Ω	186 k Ω
1400 Hz	4.7 nF	910 pF	150–250 k Ω	201 k Ω
2000 Hz	4.7 nF	470 nF	150–250 k Ω	191 k Ω
3200 Hz	2.2 nF	470 nF	68–168 k Ω	133 k Ω

II. ANALYSIS

Straightforward nodal analysis yields the transfer function of the filter in Figure 1:

$$H(s) = -\frac{b_2 s^2 + b_1 s}{a_3 s^3 + a_2 s^2 + a_1 s + 1}, \quad (1)$$

where

$$b_2 = R_2 R_3 C_1 C_2 + R_1 R_3 C_1 (C_2 + C_3), \quad (2)$$

$$b_1 = (R_2 + R_3) C_2 + R_3 C_1, \quad (3)$$

$$a_3 = R_1 R_2 R_3 C_1 C_2 C_3, \quad (4)$$

$$a_2 = R_1 (R_2 + R_3) C_2 C_3, \quad (5)$$

$$a_1 = R_1 (C_2 + C_3). \quad (6)$$

Although explicit expressions for the poles of (1) exist, they are cumbersome and provide little insight, and an exact closed-form expression for the peak frequency is out of reach. The transfer function simplifies conveniently under the special case of $R_1 = R_3$ and $C_1 = C_3$; placing it in a canonical form with the highest powers of the numerator and denominator having unit coefficients yields

$$H(s) = -\frac{\left[\frac{1}{R_1 C_1} + \frac{1}{R_2} \left(\frac{1}{C_1} + \frac{1}{C_2} \right) \right] \left(s^2 + \frac{1}{R_1 C_1} s \right)}{s^3 + \frac{1}{R_1 C_1} s^2 + \frac{1}{R_1 R_2 C_1 C_2} s + \frac{1}{R_1^2 R_2 C_1^2 C_2}}, \quad (7)$$

which can be factored as

$$H(s) = -\frac{\left[\frac{1}{R_1 C_1} + \frac{1}{R_2} \left(\frac{1}{C_1} + \frac{1}{C_2} \right) \right] \left(s + \frac{1}{R_1 C_1} \right)}{\left(s + \frac{1}{R_1 C_1} \right) \left(s^2 + \frac{1}{R_2 C_1} s + \frac{1}{R_1 R_2 C_1 C_2} \right)}. \quad (8)$$

The zero at $-1/(R_1 C_1)$ cancels with the corresponding pole, leaving the classic bandpass filter form

$$H(s) = -\frac{\frac{A \omega_n}{Q}}{s^2 + \frac{\omega_n}{Q} s + \omega_n^2}, \quad (9)$$

where

$$A = \frac{1}{R_2 R_1} + \left(1 + \frac{C_1}{C_2} \right), \quad (10)$$

$$\omega_n = \frac{1}{\sqrt{R_1 R_2 C_1 C_2}}, \quad (11)$$

$$Q = \sqrt{\frac{R_2 C_1}{R_1 C_2}}, \quad (12)$$

with a peak at ω_n , and a magnitude of A at the peak.

III. EXAMPLE

Figure 3 presents a simplified schematic² of the Buchla Model 295 10 Channel Comb Filter.³ The lowest and highest channels of the filterbank consist of three-pole Sallen-Key lowpass (Figure 4, for frequencies less than 100 Hz) and highpass (Figure 5, for frequencies higher than 7 kHz) filters, respectively. (Since this paper assumes the opamps are ideal, elements in the negative feedback loops of Figures 4 and 5 intended to deal with nonideal opamp effects have been omitted for clarity.) The middle eight bands are implemented via Figure 1, with $R_1 = 15$ k Ω for all eight and capacitances given in Table I. R_2 for each filter consists of a fixed resistor (68 k Ω for 200 Hz, 91 k Ω for 350 Hz, etc.) in series with a 100 k Ω potentiometer wired as a variable resistor, so R_2 in Table I is given as a range. R_3 for each filter is a 20 k Ω potentiometer wired as a variable resistor.

An inverting opamp configuration at the input multiplies the incoming signals by $(39 \text{ k}\Omega)/(33 \text{ k}\Omega)$. Note that a second opamp in an inverting unity gain configuration flips the signs of the input signal of the highpass filter and every-other bandpass filter; we will discuss the rationale for this in Section III-B.

The input signals for the highest and lowest channels enter their respective Sallen-Key filters directly. The input signals for the 350 Hz and 2 kHz bandpass filters are first attenuated by a voltage division factor of $(330 \text{ }\Omega)/(3.3 \text{ k}\Omega + 150 \text{ }\Omega + 330 \text{ }\Omega)$, while the input signals for the remaining bandpass filters are first attenuated by a voltage division factor of $(150 \text{ }\Omega + 330 \text{ }\Omega)/(3.3 \text{ k}\Omega + 150 \text{ }\Omega + 330 \text{ }\Omega)$. The validity of these calculations presumed that the input impedances of the various filter stages are sufficiently high, relative to various combinations of resistances in the attenuation ladder, that they could be neglected.

Outputs of all ten individual filters are available to the user through 220 Ω short-circuit protection resistors in series with the outputs of the operational amplifiers. The individual outputs, after the 220 Ω resistors, are fed to the tops of 50 k Ω slider potentiometers, wired as volume controls with the bottoms hooked to ground. The signals at the wipers of the potentiometers are summed via an operational amplifier in an inverting mixer configuration, with a feedback resistance of 56 k Ω . For the 200 Hz and 2 kHz channels, the resistors from the wipers to the virtual ground are 39 k Ω , whereas they are 33 k Ω for the remaining bands. The remaining discussion will assume that the sliders are turned all the way up. There is a slight loss in voltage from taking the inputs to the volume controls from after the 220 Ω instead of directly from the outputs of the filter opamps, but this amounts to only around 1%, so we will neglect that effect.

²The original schematic was found at https://rubidium.se/magnus/synths/companies/buchla/Buchla_2950_200.jpg (last accessed December 29, 2022); it was also found mirrored at <http://fluxmonkey.com/historicBuchla/295-10chanfilt.htm>.

³On the schematic, the designer wrote “trim 3.5 kc section @ 3.2 kc;” so we will treat the filter marked 3.5 kHz on the front panel and on the schematic as if it was intended to be 3.2 kHz. One might conjecture that the designer changed their mind about the filterbank design over the lifetime of the product, but the front panels had already been manufactured to read 3.5 kHz.

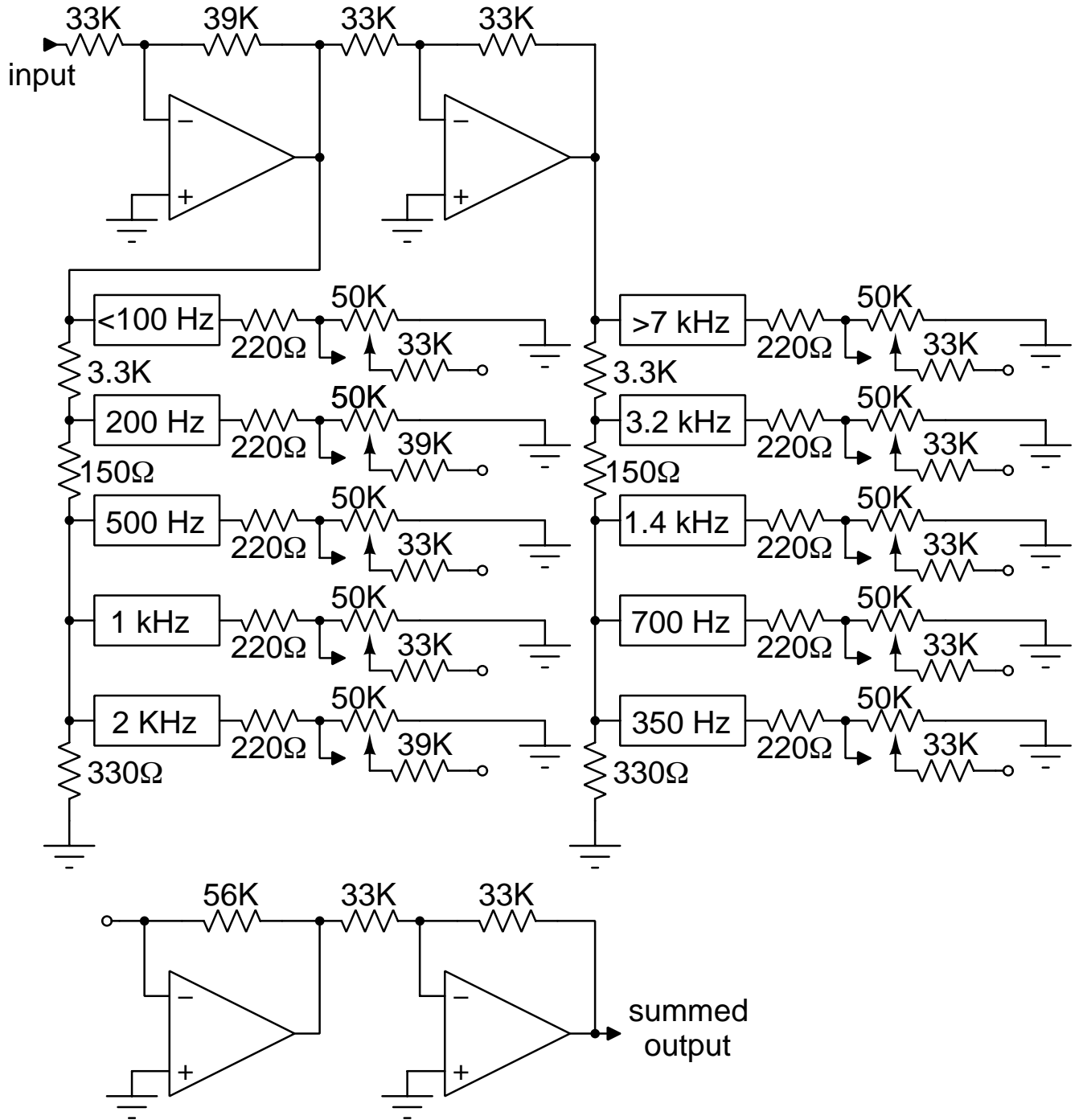


Fig. 3. Simplified schematic of the Buchla Model 295 10 Channel Comb Filter. Capital K in resistance markings represents $k\Omega$ throughout the figures. The open circles represent connections from the $33\text{ k}\Omega$ and $39\text{ k}\Omega$ summing resistors to the virtual ground of the opamp in the lower left corner. The right-facing arrows between the $220\ \Omega$ and $50\text{ k}\Omega$ resistances represent individual channel outputs. The analysis in this paper assumes the opamps are ideal, so some components meant to address nonideal opamp effects have been omitted for clarity, namely resistors between the positive input terminals of opamps and ground and DC blocking capacitors in series with the $33\text{ k}\Omega$ resistors at the initial input and connecting the bottom two opamps.

A. Calibration

As an initial estimate for choosing R_2 , if we assume $R_3 = R_1 = 15\text{ k}\Omega$, we could use (11) to compute a candidate value according to the target peak frequency f_c given in the left column of Table I: $R'_2 = 1/(2\pi f_c R_1 C_1 C_2)$. Comparing the right two columns of Table I, we see that the computed

R'_2 values are within the range allowed by the potentiometer. Letting $R_2 = R'_2$ yields the magnitude frequency responses shown in Figure 6, using equations from p. 30 of [11] for the Sallen-Key filters.

On the Buchla Model 295 schematic, the designer wrote instructions to trim each channel to achieve 6.5 dB of gain at

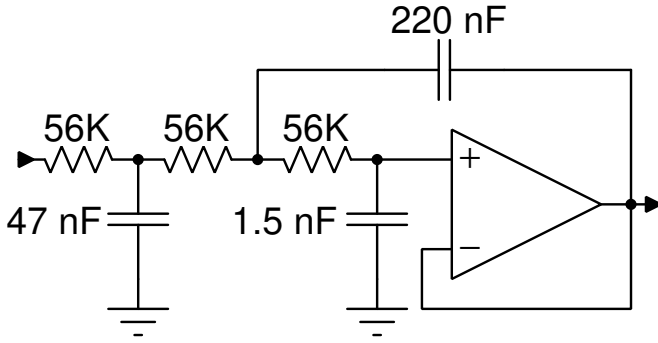


Fig. 4. Lowpass Sallen-Key filter for the below-100 Hz channel.

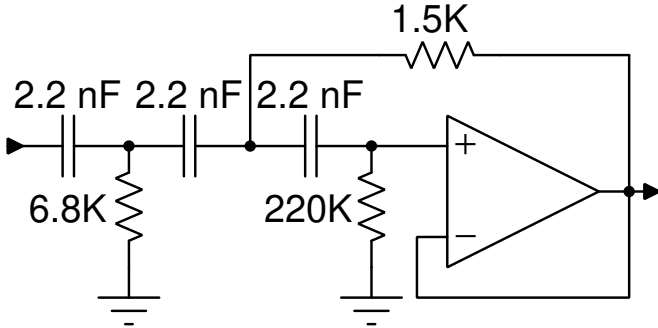


Fig. 5. Highpass Sallen-Key filter for the above-7 kHz channel.

the target frequency with the sliders set to maximum volume. They also wrote that the “100K trimmers tune frequencies,” and the “20K trimmers tune Qs (and gains).” Unfortunately, it is not so simple, as all of those quantities are effected by both trimmers. We iteratively adjusted the potentiometers by alternately changing the 20 k Ω trimmer to achieve the desired gain and the 100 k Ω trimmer to achieve the desired peak frequency, until the peaks were within 1 Hz and 0.01 dB of the desired targets. The resulting R_2 and R_3 values are given in Table II, with the corresponding frequency responses illustrated in Figure 7.

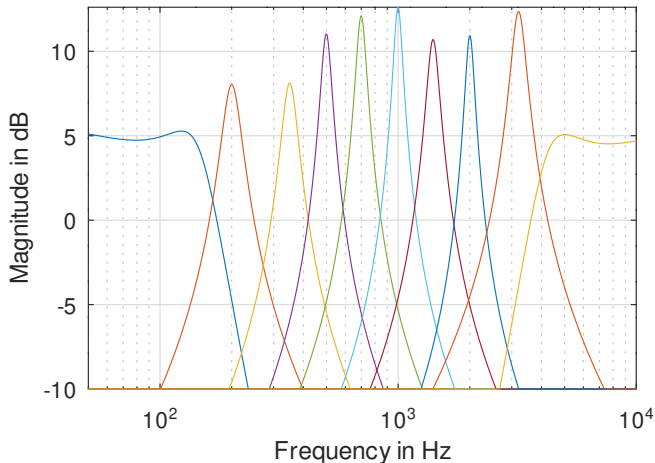
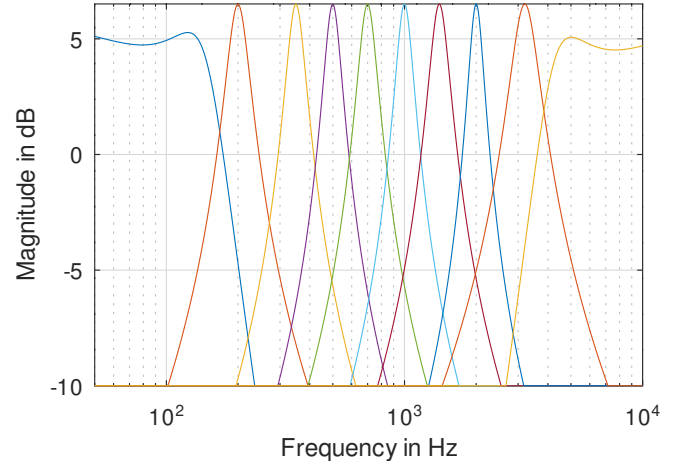
Fig. 6. Frequency responses of the 10 channels assuming $R_2 = R'_2$ and $R_3 = R_1$.Fig. 7. Frequency responses of the 10 channels assuming the R_2 and R_3 values specified in Table II.

TABLE II
BUCHLA MODEL 295 FILTERBANK CALIBRATION RESULTS

Band	R_2	R_3	Q
200 Hz	93 k Ω	13.98 k Ω	4.522
350 Hz	136.6 k Ω	14.04 k Ω	5.395
500 Hz	149.5 k Ω	13.15 k Ω	5.941
700 Hz	242 k Ω	12.41 k Ω	5.422
1000 Hz	199.5 k Ω	12.75 k Ω	5.989
1400 Hz	209.8 k Ω	12.74 k Ω	5.222
2000 Hz	200.5 k Ω	13.4 k Ω	6.946
3200 Hz	171.2 k Ω	11.3 k Ω	3.721

If the denominators of the resulting transfer functions are factored as $(s + a)[s + (\omega_n/Q) + \omega_n^2]$, where a is real, we find $\omega_n/(2\pi)$ values within 1 Hz of the target frequencies. This suggests that the complex poles and the zero at the origin dominate the response, even though the real pole does not exactly cancel with the negative real zero as in (8). Table II lists the corresponding Q values.

B. Summed Output

Figure 8 shows the summed output of all 10 channels, with all sliders at full volume. The thin solid line illustrates what happens if we ignore the opamp in the upper right corner of Figure 3, which inverts the highpass channel and every-other bandpass channel. The thick dotted line shows the result when we include those counterintuitive inversions, and illustrates why they are there. The phase responses of the neighboring filters naturally conspire to produce some wide amplitude variations, which are somewhat smoothed by inverting some of the channels. The resulting frequency response is still not particularly flat; the Buchla Model 295 is a musical effect, not a precision equalizer.

IV. CONCLUSION

We do not know, at present, where else the topology of Figure 1 may have been used, or why the designer of the Model 295 chose it over the cascaded three-pole Sallen-Key filters used in the Mosdel 294 4 Channel Comb Filter or the cascaded multiple feedback bandpass filters employed in the

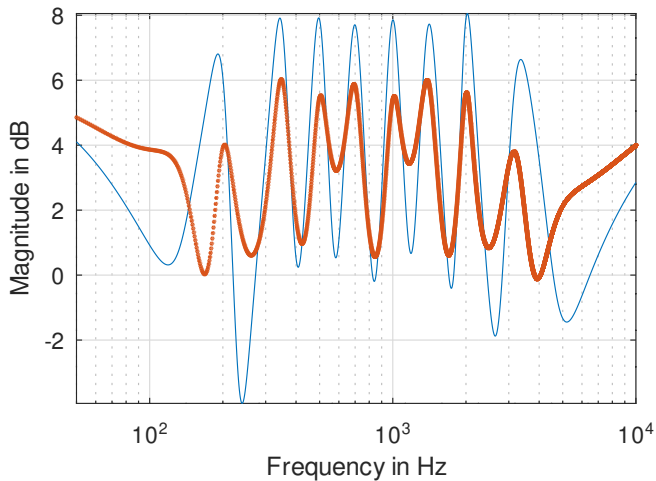


Fig. 8. Frequency response of the summed output of the Buchla Model 295. The thin solid line corresponds to omitting the inversion of certain channels. The thick dotted line includes the inversions (although the dots are spaced close enough that they appear solid throughout most of the graph).

16-band Model 296 Programmable Spectral Processor. For that matter, it is unclear whether the filter truly originated with Donald Buchla (assuming he was the designer, which is likely), or may yet be found in a “quaint and curious volume of forgotten lore,” as penned by Edgar Allen Poe, despite our thorough literature search.

Future work could explore what advantages and disadvantages Figure 1 has over other bandpass filter topologies, and formulate design procedures for the filter. We were unable to reverse engineer the designer’s thought process in choosing component values; issues like the choice of $39\text{ k}\Omega$ instead of $33\text{ k}\Omega$ for two of the filters are suggestive of some trial-and-error salting-to-taste on the designer’s part.

ACKNOWLEDGMENTS

We thank Neil Johnson for finding passive version of the filter in [8], [9], Peter Singfield for finding the articles in *Wireless World* [1], [2] and his insights about the noninverting variation of the filter, and Don Tillman for finding the article in *Popular Electronics* [5] and his help in developing intuition about the Buchla Model 295, particularly the role of the inversion of some of the channels. We particularly thank Magnus Danielson for his detailed reading of a draft of this paper and his comments.

REFERENCES

- [1] F. Girling and E. Good, “Active filters 10. Uses of the parallel-T network,” *Wireless World*, pp. 231–234, May 1970.
- [2] —, “Active filters 11. More on the parallel-T network,” *Wireless World*, pp. 285–287, June 1970.
- [3] G. Daryanani, *Principles of Active Network Synthesis and Design*. Wiley, 1976.
- [4] L. Huelsman, *Theory and Design of Active RC Circuits*. McGraw-Hill, 1968.
- [5] J. Simonton, “Build the waa-waa,” *Popular Electronics*, pp. 45–51, January 1970.
- [6] E. Zwicker, “Subdivision of the audible frequency range into critical bands,” *Journal of the Acoustical Society of America*, vol. 33, no. 2, p. 248, 1961.
- [7] M. Vail, *Vintage Synthesizers: Pioneering Designers, Groundbreaking Instruments, Collecting Tips, Mutants of Technology*, 2nd ed. Backbeat, 2000.
- [8] A. Sedra and P. Brackett, *Filter Theory and Design: Active and Passive*. Matrix Publications, 1978.
- [9] T. Watson, “Active band-pass filters using twin-tee networks,” Master’s thesis, University of Missouri at Rolla, Rolla, MO, 1965.
- [10] B. Carter, “Twin T band pass filter calculator,” http://earmark.net/gesr/opamp/twint_bpf.htm, last accessed Nov. 18, 2024.
- [11] W. Leach, “Dr. Leach’s filter potpourri,” <https://leachlegacy.ece.gatech.edu/ece4435/filtrpot.pdf>, last accessed Nov. 18, 2024.